much lower than that of the belief-propagation algorithm. Hence, we conclude by noting that the proposed algorithm achieves a performance near to or even better than that of the belief-propagation algorithm, while with a lower computational complexity.

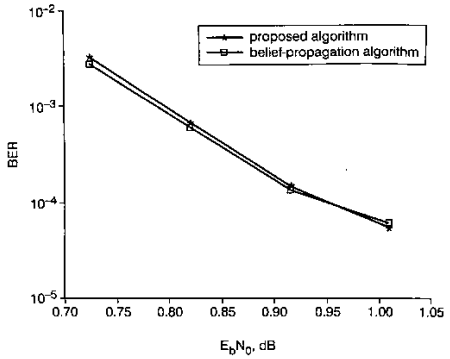

Fig. 1 *Performance of irregular LDPC code over BIAWGN channels*

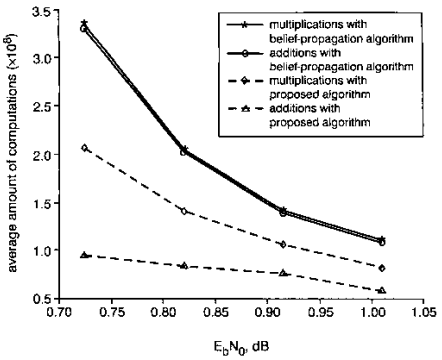

Fig. 2 *Comparison of proposed algorithm with belief-propagation algorithm in terms of decoding computations*

Conclusion: We have proposed a modified belief-propagation algorithm for decoding of irregular LDPC codes. This algorithm is very efficient and effective, providing a more practical decoding scheme for irregular LDPC codes.

Acknowledgments: This work was supported in part by the National Science Foundation (60132010) and the National Fundamental Research Program (G1998030406).

31 July 2002
Electronics Letters Online No: 20021052
DOI: 10.1049/el:20021052

Liuguo Yin, Jianhua Lu and Youshou Wu (*Department of Electronic Engineering, Tsinghua University, Beijing 100084, China*)

Khaled Ben Letaief (*Department of EEE, HKUST, Clear Water Bay, Kowloon, Hong Kong, China*)

References

1 LUBY, M., *et al.*: 'Improved low-density parity-check codes using irregular graphs', *IEEE Trans. Inf. Theory*, 2001, **47**, (2), pp. 585–598
2 THOMAS, J., SHOKROLLAHI, A., and URBANKE, R.: 'Design of capacity-approaching irregular low-density parity-check codes', *IEEE Trans. Inf. Theory*, 2001, **47**, (2), pp. 619–637
3 FAN, J.L.: 'Constrained coding and soft iterative decoding' (Kluwer Academic Publishers, 2001)

Space-time IQ-interleaved TCM and TTCM for AWGN and Rayleigh fading channels

S.X. Ng and L. Hanzo

Space-time block coded inphase-quadrature phase (IQ)-interleaved trellis coded modulation (TCM) and turbo TCM (TTCM) schemes are proposed, which are capable of quadrupling the diversity order of conventional symbol-interleaved TCM and TTCM schemes. The increased diversity order of the proposed schemes provides significant coding gains, when communicating over non-dispersive Rayleigh fading channels without compromising the coding gain achievable over Gaussian channels.

Introduction: Trellis coded modulation (TCM) [1, 2] was originally designed for transmission over additive white Gaussian noise (AWGN) channels, where it is capable of achieving coding gain without bandwidth expansion. Turbo TCM (TTCM) [2, 3] is a more recent bandwidth-efficient transmission scheme, which has a structure similar to that of the family of binary turbo codes, distinguishing itself by employing TCM schemes as component codes. Both the TCM and TTCM schemes employed set partitioning-based signal labelling, in order to increase the minimum Euclidean distance between the encoded information bits. Symbol interleavers were utilised both far the turbo interleaver and for the channel interleaver, for the sake of achieving time diversity when communicating over Rayleigh fading channels.

It was shown in [4] that the maximisation of the minimum Hamming distance measured in terms of the number of different symbols between any two transmitted symbol sequences is the key design criterion for TCM schemes contrived for flat Rayleigh fading channels, in particular when communicating at high signal-to-noise ratios (SNRs). In an effort to increase the achievable time diversity, a multidimensional TCM scheme utilising one symbol interleaver and two encoders was proposed in [5], where the individual encoders specify the inphase (I) and quadrature phase (Q) components of the complex transmitted signal, respectively. Another TCM scheme using constellation rotation was proposed in [6], which utilised two separate channel interleavers for interleaving the I and Q components of the complex transmitted signals, but assumed the absence of I/Q cross-coupling, when communicating over complex fading channels.

ST-IQ TCM/TTCM: To improve the performance of the existing state-of-the-art systems, in this Letter we propose the navel system shown in Fig. 1 which consists of space-time block codes (STBC) [7] and an IQ-interleaved TCM/TTCM scheme using no constellation rotation. We consider two transmitters and one receiver for the space time (ST) scheme and two independent IQ interleavers for the TCM/TTCM arrangement, as shown in the block diagram of Fig. 1. We denote the IQ-interleaved modulated signal by $\tilde{s} = \tilde{s}_I + j\tilde{s}_Q$, which is transmitted over the flat Rayleigh fading channel having a complex fading coefficient of $h = \alpha e^{j\theta}$ with the aid of two STBC transmitters. During the first symbol period the signals $x_1 = \tilde{s}_1$ and $x_2 = \tilde{s}_2$ are transmitted, while during the second symbol period the signals $-x_2^*$ and x_1^* are emitted from the transmit antennas 1 and 2, respectively. We assume that the fading envelope and phase are constant across the two time slots. The signal is also contaminated by the zero-mean AWGN n exhibiting a variance of $\sigma^2 = N_0/2$, where N_0 is the single-sided noise power spectral density. It can be shown that the two signals received during the two consecutive symbol periods can be represented in matrix form as $\mathbf{r} = \mathbf{A} \cdot \mathbf{x} + \mathbf{n}$:

$$\begin{pmatrix} r_1 \\ r_2^* \end{pmatrix} = \begin{pmatrix} h_1 & h_2 \\ h_2^* & -h_1^* \end{pmatrix} \begin{pmatrix} x_1 \\ x_2 \end{pmatrix} + \begin{pmatrix} n_1 \\ n_2^* \end{pmatrix}$$

where $\mathbf{A}$ is termed the system matrix. Note that the I (or Q) component of the received signal r_i, namely $r_{i,I}$ (or $r_{i,Q}$) where $i \in \{1, 2\}$, is dependent on both the I and Q components of x_1 and x_2, namely on $x_{1,I}$, $x_{1,Q}$, $x_{2,I}$ and $x_{2,Q}$, due to the cross-coupling effect imposed by the complex channel. It is, however, desirable to decouple them, so that we can compute the I (or Q) branch metrics m_I (or m_Q) in Fig. 1 for a particular x_i independently, against only $x_{1,I}$ and $x_{2,I}$ (or $x_{1,Q}$ and $x_{2,Q}$). Observe that the decoupling operation has been carried out during the STBC decoding, where the received vector $\mathbf{r}$ is multiplied with the

conjugate transpose of $\mathbf{A}$, namely with $\mathbf{A}^H$, yielding $\hat{\mathbf{x}} = \mathbf{A}^H \cdot \mathbf{r}$:

$$\begin{pmatrix} \hat{x}_1 \\ \hat{x}_2 \end{pmatrix} = (\alpha_1^2 + \alpha_2^2) \begin{pmatrix} x_1 \\ x_2 \end{pmatrix} + \mathbf{N}$$

where $\mathbf{N}$ contains the resultant noise. More specifically, the signal $\hat{x}_1 = (\alpha_1^2 + \alpha_2^2)x_1$ is the decoupled version of r_1, where $\hat{x}_{1,I}$ (or $\hat{x}_{1,Q}$) is independent of $x_{1,Q}$ and $x_{2,Q}$ (or $x_{1,I}$ and $x_{2,I}$). Hence, it can be readily shown that the associated IQ branch metrics of the STBC coded signal x_1 can be derived from $\hat{x}_1 = \hat{x}_{1,I} + j\hat{x}_{1,Q}$ as:

$$\tilde{m}_I(x_{1,I}|\hat{x}_{1,I}, D_I) = -\frac{(\hat{x}_{1,I} - D_I x_{1,I})^2}{2\sigma^2 D_I}$$

and

$$\tilde{m}_Q(x_{1,Q}|\hat{x}_{1,Q}, D_Q) = -\frac{(\hat{x}_{1,Q} - D_Q x_{1,Q})^2}{2\sigma^2 D_Q}$$

where we have $D_I = D_Q = D = (\alpha_1^2 + \alpha_2^2)$. The branch metric for x_2 is similarly computed. The effect of the associated second-order transmit diversity can be observed in the context of the term $(\alpha_1^2 + \alpha_2^2)$. Note that $\tilde{m}_I$ and $\tilde{m}_Q$ share the same D value for the same transmitted signal of $x(=\bar{s})$, but after the IQ deinterleaver of Fig. 1 m_I and m_Q will be associated with a different D value. The branch metric of the TCM/TTCM-coded signal s is computed from $m(s) = m_I(x_I = s_I) + m_Q(x_Q = s_Q)$. Since there are two independent IQ co-ordinates for a complex TCM/TTCM symbol, and since they are independently interleaved, m_I and m_Q provide independent diversity for a particular symbol. More explicitly, since we have $D_I \neq D_Q$, the IQ-interleaved TCM/TTCM scheme is expected to double the achievable diversity order compared to its symbol-interleaved counterpart. For a single-transmitter scheme, the corresponding IQ branch metric $\tilde{m}_I$ and $\tilde{m}_Q$ can be computed from that of the STBC scheme using $D = \alpha^2$ and $\mathbf{A} = h$.

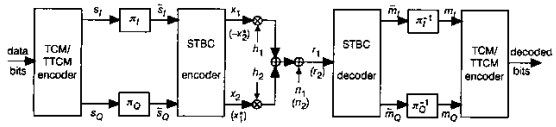

Fig. 1 *Block diagram of ST-based IQ-interleaved system*

π and π^{-1} denote interleaver and deinterleaver, respectively, $(\cdot)$ denotes STBC signals during second symbol period

Simulation results: We evaluated the performance of the proposed schemes using 16-level quadrature amplitude modulation (16QAM) in the context of both the non-iterative 64-state TCM scheme [1] and that of the iterative eight-state TTCM arrangement using four decoding iterations [3]. The rationale of using 64 and eight states, respectively, was that the TCM and TTCM schemes considered here exhibit a similar decoding complexity expressed in terms of the total number of trellis states, since there are two eight-state TTCM decoders, which are invoked in four iterations, yielding a total of $2 \times 8 \times 4 = 64$ TTCM trellis states. The effective throughput was 3 bits per symbol (BPS) in both cases.

Fig. 2 shows bit error ratio (BER) against signal-to-noise ratio per bit, namely E_b/N_0, performance of 16QAM-based ST-IQ TCM, IQ TCM, ST TCM, conventional TCM as well as that of uncoded eight-level phase-shift keying (8PSK), for transmission over uncorrelated flat Rayleigh fading channels. Again, all of the TCM schemes had an effective throughput of 3 BPS. Although it is not explicitly shown owing to lack of space, we found that all the TCM schemes exhibit a similar performance to each other in AWGN channels. By contrast, when communicating over uncorrelated flat Rayleigh fading channels, the BER curve of IQ TCM merged with that of ST TCM in the high-SNR region of Fig. 2, since they both exhibit twice the diversity potential compared to conventional TCM. As seen in Fig. 2, with the advent of ST-IQ TCM a further 6 dB gain can be obtained at a BER of 10^{-5} compared to the IQ TCM and ST TCM schemes.

By contrast, in Fig. 3 we show the BER against E_b/N_0 performance of the 16QAM-based TTCM schemes, namely that of ST-IQ TTCM, IQ TTCM, ST TTCM, conventional TTCM as well as that of uncoded 8PSK, for transmission over uncorrelated flat Rayleigh fading channels. Again, a similar performance trend is observed to that of the TCM schemes of Fig. 2, although the achievable diversity/coding gain of TTCM is smaller than that of TCM due to the fact that TTCM has achieved part of its attainable diversity gain with the aid of its iterative turbo decoding. Nonetheless, at a BER of 10^{-5}, the performance of ST-IQ TTCM is about 5.1 dB better than that of the conventional TTCM scheme.

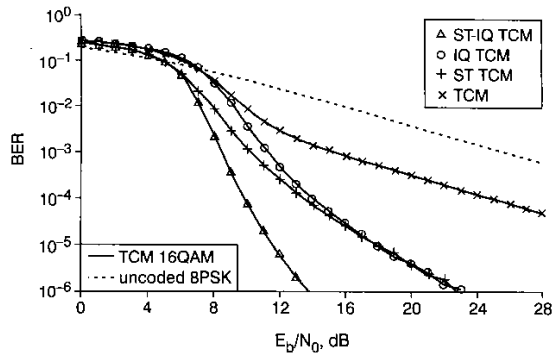

Fig. 2 *BER against E_b/N_0 performance of 16QAM-based ST-IQ TCM, IQ TCM, ST TCM, conventional TCM and uncoded 8PSK*

All of these TCM schemes have effective throughput 3 BPS

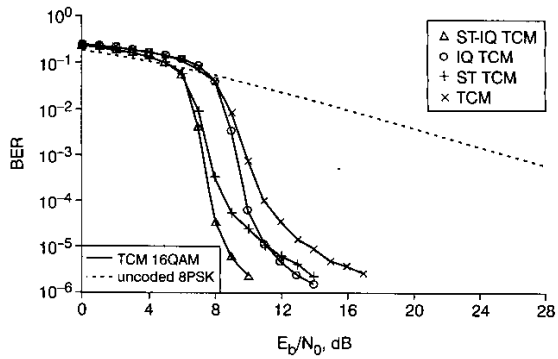

Fig. 3 *BER against E_b/N_0 performance of 16QAM-based ST-IQ TTCM, IQ TTCM, ST TTCM, conventional TTCM and uncoded 8PSK*

All of these TTCM schemes have effective throughput of 3 BPS

Conclusions: We have proposed the novel ST-IQ and IQ TCM/TTCM schemes for transmissions over both AWGN and flat Rayleigh fading channels. Both the ST-IQ TCM and ST-IQ TTCM schemes are capable of providing significant diversity gains over their conventional counterparts. Specifically, in case of uncorrelated flat Rayleigh fading channel, coding gains of 26.1 and 28.2 dB were achieved over uncoded 8PSK at a BER of 10^{-4}, respectively. For systems requiring the reduced complexity of a single-transmitter scheme, IQ TCM/TTCM is still capable of doubling the achievable diversity potential of TCM/TTCM with the aid of a single transmit antenna.

5 July 2002
Electronics Letters Online No: 20021069
DOI: 10.1049/el:20021069

S.X. Ng and L. Hanzo (*Department of Electronics and Computer Science, University of Southampton, Southampton SO17 1BJ, United Kingdom*)

E-mail: lh@ecs.soton.ac.uk

References

1 UNGERBÖCK, G.: 'Channel coding with multilevel/phase signals', *IEEE Trans. Inf. Theory*, 1982, **28**, pp. 55–67

2 HANZO, L., LIEW, T.H., and YEAP, B.L.: 'Turbo coding, turbo equalisation and space time coding for transmission over wireless channels' (John Wiley IEEE Press, New York, 2002)

3 ROBERTSON, P., and WÖRZ, T.: 'Bandwidth-efficient turbo trellis-coded modulation using punctured component codes', *IEEE J. Sel. Areas Commun.*, 1998, **16**, pp. 206–218
4 DIVSALAR, D., and SIMON, M.K.: 'The design of trellis coded MPSK for fading channel: performance criteria', *IEEE Trans. Commun.*, 1988, **36**, pp. 1004–1012
5 AL-SEMARI, S., and FUJA, T.: 'I-Q TCM: reliable communication over the Rayleigh fading channel close to the cuttoff rate', *IEEE Trans. Inf. Theory*, 1997, **43**, pp. 250–262
6 JELICIC, B.D., and ROY, S.: 'Design of trellis coded QAM for flat fading and AWGN channels', *IEEE Trans. Veh. Technol.*, 1994, **44**, pp. 192–201
7 ALAMOUTI, S.M.: 'A simple transmitter diversity scheme for wireless communications', *IEEE J. Sel. Areas Commun.*, 1998, **16**, pp. 1451–1458

Generation of ultra-high repetition rate optical pulse bursts by means of fibre Bragg gratings operating in transmission

J. Azaña, R. Slavík, P. Kockaert, L.R. Chen and S. LaRochelle

An experimental demonstration of the use of specially apodised, linearly chirped fibre Bragg gratings operating in transmission for generating a customised ultra-high repetition rate optical pulse burst (325 GHz, in the example shown) from a single ultra-short pulse.

Introduction: Generation of optical pulse bursts at repetition rates beyond those achievable by conventional modelocking techniques is becoming increasingly important for many areas, including ultra-high-speed optical communications, photonic signal processing, and optical computing. Ultra-high repetition rate pulse bursts can be generated by amplitude/phase spectral filtering of a single ultra-short input pulse using pulse shaping techniques based on bulk optics [1], integrated arrayed waveguide gratings [2], or fibre Bragg gratings (FBGs) [3–5]. The advantages of FBGs over other technologies are inherent to an all-fibre approach: compactness, low insertion loss, and the potential for low cost.

In this Letter we experimentally demonstrate the use of specially apodised linearly chirped FBGs (LCFBGs) operating in transmission as amplitude filtering stages for generating a customised ultra-high repetition rate optical pulse burst from a single ultra-short input pulse, or alternatively from a lower rate pulse sequence. In particular, we use a single apodised LCFBG specifically designed to generate a 325 GHz optical pulse burst by transmission of two identical narrow spectral bands. This technique offers all the advantages of an FBG-based solution and in addition avoids the use of additional devices (e.g. optical circulators or Mach-Zehnder interferometers) to retrieve the reflected and processed signals.

Principle of operation: High repetition rate optical pulse bursts can be produced by amplitude/phase spectral filtering of a single ultra-short input pulse [1]. In general, the required filter must be spectrally periodic in both amplitude and phase. Amplitude-only and phase-only filtering represent two extremes. In the amplitude-only filtering approach, a periodic set of frequency components of the original pulse is blocked, the group delay of the periodic filter is constant within each period and all passbands experience the same group delay. This results in a periodic pulse train the repetition rate of which is equal to the frequency spacing of the filter bands. Furthermore, the amplitude response within one spectral period of the filter determines the shape of the temporal envelope of the generated pulse burst.

All-fibre periodic amplitude filters can be implemented using sampled or superimposed FBG structures operating in reflection [3, 5], or FBG-based Fabry-Perot (FP) cavities operating in transmission [6]. The FP approach presents the advantages of a large number of transmission peaks [6]. However, the spectral passbands in an FP filter always exhibit a Lorentzian shape, which would result in a rapidly decaying temporal envelope for the burst, causing undesirable pulse-to-pulse intensity fluctuations.

Alternatively, we show in this Letter that all-fibre periodic amplitude filters can be implemented using a single specially apodised LCFBG operating in transmission. Consider an apodised LCFBG with a constant effective refractive index n_{av}, a period chirp C_Λ, and an apodisation profile $A(z)$ (z is along the fibre axis). As shown in [7], the apodisation profile $A(z)$ can be 'mapped' into the magnitude of its complex transmission coefficient $|H_t(\lambda)|$ (so-called space-to-wavelength mapping):

$$|H_t(\lambda')| \propto 1 - A\left(z = \frac{\lambda'}{2n_{av}C_\Lambda}\right), \quad 0 \le z \le L \tag{1}$$

where $\lambda' = \lambda - \lambda_0$ (with λ_0 being the Bragg wavelength at the input end of the grating, $z = 0$), and L is the grating length. However, an efficient space-to-wavelength mapping is ensured only if the following condition is verified [7]

$$|C_\Lambda| \ll K\Delta\lambda^2 \tag{2}$$

where K is a constant dependent on the shape of the apodisation profile and $\Delta\lambda$ is the single passband bandwidth. As a consequence of (2), the choice of the grating chirp is limited by the bandwidth which has to be resolved (the narrower the bandwidth, the lower the grating chirp). Since we operate the grating in transmission where the group delay is constant within each transmitted spectral band (neglecting fibre dispersion) and all the bands experience the same group delay, we are performing an amplitude-only filtering process.

Note that we also have high flexibility in tailoring the spectral shape of the passbands, which is essential to control the temporal envelope of the generated pulse burst: as discussed above, we only need to record the desired spectral shape in the grating apodisation profile (see (1)).

Results and discussion: For our experiments, we used a single apodised LCFBG specifically designed to generate a 325 GHz optical pulse burst. For simplicity, we consider here only two transmitted bands but of course the grating can be similarly designed to transmit a larger number of spectral bands. The apodised LCFBG was written using a phase-mask scanning method with dithering to realise the apodisation profile [8]. The phase mask (Teraxion Inc.) had a chirp of 1.25 nm/cm ($C_\Lambda = 0.625$ nm/cm). To satisfy the condition expressed in (2) with the available phase mask, the repetition rate needed to be more than 300 GHz (to obtain a lower repetition rate, a phase mask with lower chirp would be necessary). The grating was ≃49 mm long, which ensures that the grating reflection bandwidth (≃9 nm) is broader than that of the input pulse (≃5 nm). The apodisation profile of the LCFBG (Fig. 1, inset) consists of two separate valleys which, by virtue of the space-to-wavelength mapping process, translates into two transmitted spectral bands. The amplitude shape of these bands was optimised using numerical simulations [5] to achieve an approximately square-like temporal envelope for the generated pulse burst. To achieve the desired repetition rate, the spectral separation between transmitted bands must be ≃2.57 nm (≃325 GHz), i.e. using (1), a spatial separation between the valleys in the apodisation profile of ≃13.7 mm is required.

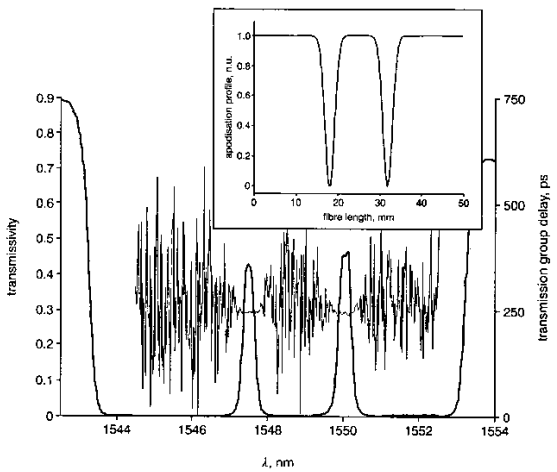

Fig. 1 *Measured transmission characteristics of FBG*
—— transmissivity – – – transmission group delay
Inset: Apodisation profile of FBG